JPn Neuroscience

The Journal of Physiology

J Physiol 593.19 (2015) pp 4453–4469

μ opioid receptor activation hyperpolarizes respiratory-controlling Kölliker–Fuse neurons and suppresses post-inspiratory drive

Erica S. Levitt[1], Ana P. Abdala[2], Julian F. R. Paton[2], John M. Bissonnette[3] and John T. Williams[1]

[1] *Vollum Institute, Oregon Health and Science University, Portland, OR 97239, USA*
[2] *School of Physiology and Pharmacology, University of Bristol, Bristol BS8 1TD, UK*
[3] *Department of Obstetrics and Gynecology, Oregon Health and Science University, Portland, OR 97239, USA*

Key points

- In addition to reductions in respiratory rate, opioids also cause aspiration and difficulty swallowing, indicating impairment of the upper airways. The Kölliker–Fuse (KF) maintains upper airway patency and a normal respiratory pattern.
- In this study, activation of μ opioid receptors in the KF reduced respiratory frequency and tidal volume in anaesthetized rats.
- Nerve recordings in an *in situ* preparation showed that activation of μ opioid receptors in the KF eliminated the post-inspiration phase of the respiratory cycle.
- In brain slices, μ opioid agonists hyperpolarized a distinct population (61%) of KF neurons by activation of an inwardly rectifying potassium conductance.
- These results suggest that KF neurons that are hyperpolarized by opioids could contribute to opioid-induced respiratory disturbances, particularly the impairment of upper airways.

Abstract Opioid-induced respiratory effects include aspiration and difficulty swallowing, suggesting impairment of the upper airways. The pontine Kölliker–Fuse nucleus (KF) controls upper airway patency and regulates respiration, in particular the inspiratory/expiratory phase transition. Given the importance of the KF in coordinating respiratory pattern, the mechanisms of μ opioid receptor activation in this nucleus were investigated at the systems and cellular level. In anaesthetized, vagi-intact rats, injection of opioid agonists DAMGO or [Met^5]enkephalin (ME) into the KF reduced respiratory frequency and amplitude. The μ opioid agonist DAMGO applied directly into the KF of the *in situ* arterially perfused working heart–brainstem preparation of rat resulted in robust apneusis (lengthened low amplitude inspiration due to loss of post-inspiratory drive) that was rapidly reversed by the opioid antagonist naloxone. In brain slice preparations, activation of μ opioid receptors on KF neurons hyperpolarized a distinct population (61%) of neurons. As expected, the opioid-induced hyperpolarization reduced the excitability of the neuron in response to either current injection or local application of glutamate. In voltage-clamp recordings the outward current produced by the opioid agonist ME was concentration dependent, reversed at the potassium equilibrium potential and was blocked by $BaCl_2$, characteristics of a G protein-coupled inwardly rectifying potassium (GIRK) conductance. The clinically used drug morphine produced an outward current in KF neurons with similar potency to morphine-mediated currents in locus coeruleus brain slice preparations. Thus, the population of KF neurons that are hyperpolarized by μ opioid agonists are likely mediators of the opioid-induced loss of post-inspiration and induction of apneusis.

DOI: 10.1113/JP270822

(Received 23 April 2015; accepted after revision 12 July 2015; first published online 15 July 2015)
Corresponding author E. S. Levitt: Vollum Institute, Oregon Health and Science University, 3181 SW Sam Jackson Park Road, Portland, OR 97239, USA. Email: levitt@ohsu.edu

Abbreviations ACSF, artificial cerebrospinal fluid; ANOVA, analysis of variance; AP, action potential; CTAP, D-Phe-Cys-Tyr-D-Trp-Arg-Thr-Pen-Thr-NH_2; CV, coefficient of variation; cVN, central vagus nerve; DAMGO, ([D-Ala^2, *N*-Me-Phe^4, Gly^5-ol]-enkephalin; DNQX, 6,7-dinitroquinoxaline-2,3-dione; E2, stage 2 expiration; GIRK, G protein-coupled inwardly rectifying potassium; KF, Kölliker–Fuse; LC, locus coeruleus; ME, [Met]^{5}enkephalin; NLX, naloxone; PB, parabrachial; PN, phrenic nerve; post-I, post-inspiration; preBötC, preBötzinger complex; scp, superior cerebellar peduncle; T_E, expiratory time; T_I, inspiratory time.

Introduction

The number of opioids prescribed per year in the USA has been steadily increasing, as have the number of deaths from opioid overdose (Chakravarthy *et al.* 2012). The primary cause of death from opioid overdose is respiratory depression. Respiration is a coordinated motor behaviour controlled by a central neural network. The brainstem respiratory network comprises a bilateral column of highly connected brain regions that stretch from the rostral pons to the caudal medulla with output to spinal and cranial motor nerves. Opioids alter breathing by activating μ opioid receptors (Dahan *et al.* 2001) located throughout the respiratory network, including areas important for inspiration (preBötzinger complex (preBötC)), expiration (Bötzinger complex), post-inspiration and phase transition (Kölliker–Fuse (KF)) and chemoreception (Lonergan *et al.* 2003; Zhang *et al.* 2007, 2011; Montandon *et al.* 2011; Prkic *et al.* 2012). The cellular effect of opioids in some of these areas has been investigated. Opioids have been shown to hyperpolarize a population of preBötC neurons in thick brain slices (Gray *et al.* 1999) and microdialysis of the opioid antagonist naloxone into the preBötC prevented the decrease in respiratory rate caused by low-dose systemic fentanyl administration to anaesthetized rats (Montandon *et al.* 2011). However, opioids also depress respiratory rate when administered to the dorsal lateral pons (which contains the KF) of dogs and cats (Hurlé *et al.* 1985; Prkic *et al.* 2012) and microinjection of naloxone into the parabrachial/KF area reversed the respiratory depression caused by systemic remifentanil in anaesthetized dogs (Prkic *et al.* 2012). In mice that endogenously express tagged μ opioid receptors, high levels of expression have been reported in the lateral parabrachial area (Erbs *et al.* 2015). Although it is well known that the pons, especially the KF, is critical for the maintenance of a eupnoeic respiratory cycle (Lumsden, 1923; Fung & St-John, 1995; Dutschmann & Herbert, 2006; Smith *et al.* 2007), the cellular mechanism for opioid-induced respiratory depression in the KF is not understood.

In addition to the well-known clinical effects of opioids on respiratory rate, tidal volume and reflex responses to hypercapnia and hypoxia, opioids also cause aspiration and difficulty swallowing (Christ *et al.* 2006; Savilampi *et al.* 2013, 2014), indicating impairment of the upper airways. The primary roles of the KF are to maintain upper airway patency and initiate post-inspiration. Ablation or pharmacological silencing of the entire KF causes apneusis, characterized by lengthened low amplitude inspiration due to the loss of the post-inspiratory drive (Lumsden, 1923; Fung & St-John, 1995; Dutschmann & Herbert, 2006; Smith *et al.* 2007). Since evidence supports the presence of μ opioid receptors in the KF, the goal of the present study was to determine the effects of μ opioid receptor activation on respiratory pattern and the cellular mechanisms that may mediate these effects. In experiments using *in situ* arterially perfused working heart–brainstem preparations of rat, microinjection of the μ opioid agonist [D-Ala^2, *N*-Me-Phe^4, Gly^5-ol]-enkephalin (DAMGO) into the KF abolished post-inspiration and caused apneusis, similar to global silencing of the KF. In whole-cell recordings of KF neurons contained in rat brain slices, activation of μ opioid receptors hyperpolarized a majority (61%) of KF neurons. The hyperpolarizing current was due to activation of a G protein-coupled inwardly rectifying potassium (GIRK) conductance. Thus, KF neurons that are hyperpolarized by opioids are additional potential mediators of opioid-induced respiratory disturbances.

Methods

Animals

Rats (Sprague–Dawley or Wistar) were used for all experiments. Animal experiments were conducted in accordance with the National Institutes of Health guidelines and with approval from the Institutional Animal Care and Use Committee of the Oregon Health and Science University (Portland, OR, USA) or performed in accordance with the European Commission Directive 86/609/EEC (European Convention for the Protection of Vertebrate Animals used for Experimental and Other Scientific Purposes) and the UK Home Office (Scientific Procedures) Act (1986) with project approval from the respective Institutional Animal Care and Use Committees.

Respiratory inductance plethysmography

Rats (Sprague–Dawley, male and female, postnatal day (P) 24–30, Charles River Laboratories, 19 rats) were anaesthetized with 1.5–2% isoflurane in 100% oxygen at a flow rate of 0.8 ml min^{-1}. Providing oxygen (100%) will maintain high blood oxygenation and decrease the risk of hypoxia during anaesthesia. However, it will also remove peripheral drive from carotid bodies. Experiments using male and female rats produced similar results, so data were pooled. A pulse transducer (MP100, AD Instruments, Colorado Springs, CO, USA) was fixed against the abdomen of the rat with a Velcro strap to measure respiratory rate and relative amplitude via inductance plethysmography. Recordings were digitized with PowerLab (ADInstruments, Chart 5 software). Rate and relative peak inspiratory and expiratory amplitudes were analysed offline with Chart 5 software.

Stereotaxic microinjections in anaesthetized rats

Rats were placed in a stereotaxic alignment system (Kopf Instruments, Tujunga, CA, USA) and the skull between bregma and lambda was levelled horizontally. A small hole was drilled in the skull at coordinates (from bregma) $x = \pm 2.1$ mm and $y = -7.5$ mm. Single-barrel glass pipettes were filled with glutamate (5 mM), ME (5 mM) or DAMGO (1 mM) diluted in normal saline. The KF was functionally identified with sequential ($z = -7.0$ to -7.7 mm) injections of glutamate (60 nl) until a brief bradypnoea or biphasic response (tachypnoea followed by prominent bradypnoea) was obtained (Chamberlin & Saper, 1994). ME or DAMGO injections (60 nl) were made at the glutamate-identified sites. Injection volumes were controlled using a Nanoject II Autoinjector (Drummond Scientific, Broomall, PA, USA). FluoSpheres 505/515 (10%; Invitrogen, Waltham, MA, USA) were included with ME or DAMGO to visualize injection sites. Injection of FluoSpheres (10%) in saline into KF had no effect on respiratory rate or relative amplitude ($n = 4$). Following the experiment the rats were killed by thoracic percussion and their brains removed and cut into horizontal slices (230 μm) using a vibrotome (Leica VT 1200S, Leica Biosystems, Buffalo Grove, IL, USA). Free-floating slices were placed in artificial cerebrospinal fluid (ACSF) and injection sites were visualized (Olympus MVX10, Olympus, Waltham, MA, USA). Experiments with missed KF injection sites based on the location of FluoSpheres were excluded. For DAMGO injections n represents number of rats ($n = 4$ rats). Since ME effects were transient, each unilateral injection was considered a separate n, and no more than two injections were used per animal (one per side) ($n = 7$ injections in 5 rats).

In situ arterially perfused working heart–brainstem preparation

Recordings from cranial and spinal nerves were performed using an *in situ* arterially perfused working heart–brainstem preparation of rats (Paton, 1996; St-John & Paton, 2000; Wilson *et al.* 2001). Since the KF circuitry of rat is mature by P15 (Dutschmann *et al.* 2009), juvenile rats (male, P24–30, $n = 14$ rats) were used. Experiments using Wistar and Sprague–Dawley rats produced similar results so data were pooled. Rats were heparinized (1000 U, I.P.) and 20 min later were deeply anaesthetized with isoflurane until visible respirations had nearly ceased. Rats were bisected below the diaphragm and decerebrated at the precollicular level in ice-cold modified Ringer solution containing (in mM): 125 NaCl, 3 KCl, 2.5 $CaCl_2$, 1.25 $MgCl_2$, 1.25 KH_2PO_4, 10 D-glucose and 24 $NaHCO_3$. The lungs and diaphragm were removed, phrenic nerves (PN) and left central vagus nerve (cVN) were isolated and cut distally, and the cerebellum was removed to allow access to the dorsal surface of the brainstem. The preparation was transferred to a recording chamber in prone position, mounted on ear bars so the brainstem was horizontal, and the descending aorta was perfused through a double lumen catheter with warmed (31–33°C), carbogenated (95% O_2–5% CO_2) modified Ringer solution containing polyethylene glycol 20,000 (1.25%) for oncotic pressure. The perfusion solution was recirculated using a peristaltic roller pump (Watson Marlow 505D, Watson Marlow, Wilmington, MA, USA) at a flow rate between 21 and 24 ml min^{-1}. Perfusion pressure was monitored using the second lumen of the aortic catheter. Vasopressin (200–400 pM) was added to maintain perfusion pressure between 60 and 90 mmHg. Vecuronium bromide (4 μg ml^{-1}, Organon Teknica, Cambridge, UK) was added to block neuromuscular transmission.

Simultaneous recordings of phrenic nerve (PN) and central vagus nerve (cVN) were obtained using bipolar glass suction electrodes (15–25 μm tip diameter). Recordings were AC amplified (A-M Systems Model 1700, A-M Systems, Carlsborg, WA, USA) at 10 kHz, band-pass filtered (300 Hz–5 kHz) and digitized at 3–10 kHz (A–D converter and Spike2 software, Cambridge Electronic Design, Cambridge, UK). Nerve activity was positively rectified and integrated (50 ms time constant) online and analysed offline with Spike2 software (Cambridge Electronic Design).

Microinjections were performed using a Kopf stereotaxic apparatus and triple-barrelled glass injection pipettes. Microinjection pipettes were filled with glutamate (5 mM), DAMGO (0.1 or 1 mM) and Evan's blue dye (2%) diluted in ACSF (Harvard Apparatus, Holliston, MA, USA). Microinjection pipettes were placed just caudal to the inferior colliculus, 2.0–2.5 mm lateral from

midline. The KF was functionally identified with sequential (dorsal to ventral) injections of glutamate (30–60 nl) until a post-inspiratory apnoea (pause in phrenic nerve firing and corresponding increase in cVN activity) was obtained, typically 2.5–3.0 mm ventral from the exposed brainstem surface (Dutschmann & Herbert, 2006). The stereotaxic coordinates of the positive injection site were recorded and the contralateral KF was identified as above. The order of left or right side identification was varied. After a baseline period (∼5 min), DAMGO (30–60 nl) was injected unilaterally. Within 5–10 min, DAMGO was injected into the contralateral KF. At the end of the experiment Evan's blue dye (30–60 nl) was injected bilaterally at the same coordinates. Injection volume was determined by visualizing the drop in the meniscus level in the pipette using a binocular microscope with a calibrated graticule eyepiece positioned perpendicular to the injection pipette. Following the experiment the brainstem was removed, fixed in 4% paraformaldehyde for at least 24 h (4°C) and stored in PBS (4°C) until further processing. Coronal slices (100 μm) containing the injection site were cut in PBS using a vibratome (Leica VT 1000S) and digitally imaged (Leica M165FC).

Brain slice electrophysiology

Recording conditions and acute brain slice preparation was performed as described previously (Levitt & Williams, 2012). Rats (Sprague–Dawley, male, 4–7 weeks) were killed by thoracic percussion and the brain was removed, blocked and mounted in a vibratome chamber (Leica VT 1200S). Horizontal or coronal slices (240 μm) were prepared in ice-cold artificial cerebrospinal fluid (ACSF) containing (in mM): 126 NaCl, 2.5 KCl, 1.2 $MgCl_2$, 2.6 $CaCl_2$, 1.2 NaH_2PO_4, 11 D-glucose and 21.4 $NaHCO_3$ (equilibrated with 95% O_2–5% CO_2). Slices were stored at 32°C in glass vials with oxygenated (95% O_2–5% CO_2) ACSF. For most experiments MK801 (10 μM) was included in the cutting and initial incubation solution to block NMDA receptor-mediated excitotoxicity. MK801 irreversibly blocks NMDA receptors, so for experiments that required NMDA receptor activity (glutamate-induced cell firing experiments) the reversible NMDA blocker kynurenic acid (1.5 mM) was used instead of MK801. After an incubation period of at least 30 min, slices were hemisected and transferred to a recording chamber which was perfused with 34°C ACSF (95% CO_2–5% O_2) at a rate of 1.5–3 ml min^{-1}.

Coronal and horizontal brain slices containing KF were used. Coronal slices were collected at the level of the inferior colliculus joining the pons (between the locus coeruleus (LC) and the dorsal raphe) containing the superior cerebellar peduncle (scp) elongated and diagonally oriented (−8.7 to −9.1 mm caudal from bregma; Paxinos & Watson, 1998). KF neurons were identified 0–500 μm ventrolateral to the tip of the scp. Horizontal slices were collected ventral to the LC when the lateral arms of the fourth ventricle were closed and the scp was not apparent (−7.8 and −7.6 mm ventral from bregma; Paxinos & Watson, 1998). The KF was identified on the lateral edge of the slice just caudal to the lateral lemniscus. The location of KF neurons in coronal and horizontal slices was consistent with the rat brain atlas (Paxinos & Watson, 1998) and functionally identified microinjection sites. For brain slice experiments each *n* represents an independent neuron and slice, and on average two slices were used per animal.

Whole-cell recordings were made from KF neurons with an Axopatch 1D amplifier in voltage-clamp (V_{hold} = −60 mV) or current-clamp mode. Recording pipettes (1.7–2.2 MΩ) were filled with internal solution containing (in mM): 115 potassium methanesulfonate, 20 KCl, 1.5 $MgCl_2$, 5 Hepes(K), 2 BAPTA, 2 Mg-ATP, 0.2 Na-GTP, pH 7.4, 275–280 mosmol l^{-1}. Liquid junction potential (10 mV) was not corrected. Data were filtered at 10 kHz and collected at 20 kHz with AxoGraphX or 400 Hz with PowerLab (Chart version 5.4.2; AD Instruments). For cell capacitance and resistance measurements, data were filtered and collected at 20 kHz with AxoGraphX. Series resistance was monitored without compensation and remained < 15 MΩ for inclusion. Cell firing data were acquired in current-clamp mode by injecting current steps (50–250 pA, 2 s). Firing frequency was reported as the average firing for the duration of the step excluding an initial burst of two to five action potentials. Action potentials from the first three steps (50, 100, 150 pA) were averaged (25–50 APs) and AP half-width and after-hyperpolarization were measured from the averaged trace.

In some experiments, glutamate was applied by iontophoresis with 50 nA negative current for 50–300 ms from thin-walled glass pipettes (50–70 MΩ) filled with glutamate (1 M, pH 8.0). A backing current of +2–4 nA was applied to prevent passive leakage. In other experiments, ME was applied by iontophoresis with 7–20 nA positive current for 2–3 s from thin-walled glass pipettes (50–70 MΩ) filled with ME (10 mM). A backing current of −2 nA was applied to prevent passive leakage. Voltage ramps (−40 to −140 mV, 500 ms) were applied immediately before and at the peak of an iontophoretic application of ME. Three sweeps were averaged, decimated in bins of 20 and baseline current was subtracted from the current at the peak of ME application to determine the ME-induced current–voltage (*I–V*) relationship. For many experiments, drugs (including CTAP, morphine, naloxone, DAMGO and ME) were applied by bath perfusion at the indicated concentrations. Bestatin (10 μM) and thiorphan (1 μM) were included with bath perfusion of ME to prevent degradation.

Neurobiotin staining

KF neurons (1–2 per slice) were filled by recording with an internal solution containing Neurobiotin (0.1%). Slices were fixed in paraformaldehyde (4%) in PBS (1 h, room temperature), washed in PBS (4°C, overnight), incubated in fetal bovine serum (10%) and Triton X-100 (0.5%) for 4 h at room temperature, incubated in Alexa Fluor 568-conjugated streptavidin (1:1000, 1 h, room temperature, Molecular Probes, Waltham, MA, USA), washed in PBS and mounted using Fluoromount (Sigma-Aldrich, St Louis, MO, USA). Images were collected on a confocal laser scanning microscope (Zeiss LSM 710) with a ×20 objective (0.8 NA).

Drugs

[Met^5]-enkephalin acetate salt (ME), [D-Ala^2, *N*-Me-Phe^4, Gly^5-ol]-enkephalin acetate salt (DAMGO), bestatin HCl, DL-thiorphan, D-Phe-Cys-Tyr-D-Trp-Arg-Thr-Pen-Thr-NH_2 (CTAP) and 6,7-dinitroquinoxaline-2,3-dione (DNQX) were from Sigma-Aldrich (St Louis, MO, USA). Morphine base was obtained from the National Institute on Drug Abuse Neuroscience Centre (Bethesda, MD, USA). Naloxone and MK801 were from Abcam (Cambridge, MA, USA). L-Glutamic acid was from Tocris (Ellisville, MO, USA). The endogenous opioid ligand ME was preferentially used because it readily washes out of the slice to allow multiple applications, and can be applied by iontophoresis. DAMGO was used when μ opioid receptor selectivity and/or peptidase-resistance was desired.

Data analysis

Plethysmography experiments were analysed using Chart 5 software. Instantaneous respiratory rate (breaths per minute) was determined off-line by detecting expiratory peaks (ratemeter noise threshold 10–15%). To determine the change in rate following opioid injection into KF, instantaneous rate was averaged for 10 breaths at the nadir of ME effect or for 2–3 min after DAMGO injection. Data from DAMGO injections into KF were used to determine inspiratory (T_I) or expiratory time (T_E). T_I (430 ± 37 ms) was measured from the beginning of inspiration (upward deflection) to the following expiratory peak (downward deflection) (Fig. 1*D*). T_E (1091 ± 262 ms) was measured from the expiratory peak to the beginning of the next inspiration. T_I and T_E were measured for 20 consecutive breaths per condition and reported as means. Statistical comparisons of rate and amplitude following ME injection compared to baseline were made using paired *t* tests of raw data. Statistical comparisons of rate, amplitude and duration of T_I and T_E following DAMGO injections compared to baseline were made using repeated measures one-way ANOVA and Bonferroni's post-test of raw data. Normalized data are shown in Fig. 1 for clarity.

Integrated nerve activity from *in situ* experiments was analysed offline with Spike2 software using custom macros. T_I, T_E and respiratory rate were determined from the integrated phrenic nerve recording. T_I was the duration of phrenic nerve activity above baseline per cycle. T_E was the duration of time that the phrenic nerve was not active above baseline per cycle. Rate was determined from the beginning of one phrenic nerve burst to the next (one complete cycle) and reported as cycles per minute. The duration of post-inspiration and stage 2 expiration (E2) were determined using integrated vagus and phrenic nerve recordings. Post-inspiration was defined as the time from the end of phrenic nerve discharge to the cessation of vagus nerve activity per cycle. The duration of E2 was defined as the time from vagus nerve quiescence (i.e. from the end of post-inspiration) to the beginning of the subsequent phrenic nerve burst. In the absence of post-inspiration, the expiratory phase was mostly or entirely E2. The coefficient of variation (SD/mean × 100) was determined for rate, T_I and T_E for each animal. All respiratory parameters were measured for at least 50 consecutive cycles per condition and reported as means. Statistical comparisons were made using repeated measures one-way ANOVA with Bonferroni's post-test of raw data. Normalized PN amplitude data are reported for clarity.

For concentration–response experiments, one or two concentrations of ME or a low concentration of ME and one concentration of DAMGO was typically tested per slice and treated as individual data points. In morphine experiments, the current produced by morphine was normalized to the current produced by ME (0.3 μM) but only one concentration of morphine (or a high concentration of ME (30 μM)) was tested per slice. Concentration–response curves were fitted with non-linear regression (constraints: Hillslope = 1, Bottom = 0). Statistical analysis was performed using GraphPad Prism 6 software (La Jolla, CA, USA). Values are presented as means ± SEM. Comparisons with $P < 0.05$ were considered significant. Data sets with $n > 15$ were tested for normality using the D'Agostino–Pearson normality test. Non-parametric statistical tests were used if one data set of a comparison failed the normality test and was not well fitted by a Gaussian frequency distribution. Statistical tests used are listed in the figure legends or in the text (for data not represented in figures).

Results

Opioids in KF/lateral parabrachial area depress respiratory drive in anaesthetized rats

To initially identify a role for the pontine respiratory group in opioid-induced respiratory depression in rats, the

endogenous opioid agonist [Met^5]enkephalin (ME) or the peptidase-resistant μ opioid agonist DAMGO was microinjected into the lateral parabrachial (PB) area, including the KF, of anaesthetized, spontaneously breathing, vagi-intact rats (n = 9 rats; Fig. 1). Respiration was monitored using inductance plethysmography (Fig. 1*A*). Relative changes in total inspiratory and expiratory amplitude were detected for each respiratory cycle. Baseline respiratory rate was 66 ± 10 breaths min^{-1}.

The KF/lateral PB was functionally identified with sequential stereotaxic injections of glutamate (5 mM, 60 nl) until a brief reduction of rate or biphasic change of rate (tachypnoea followed by prominent bradypnoea) was obtained (average reduction of rate = 28 ± 7%; P = 0.002

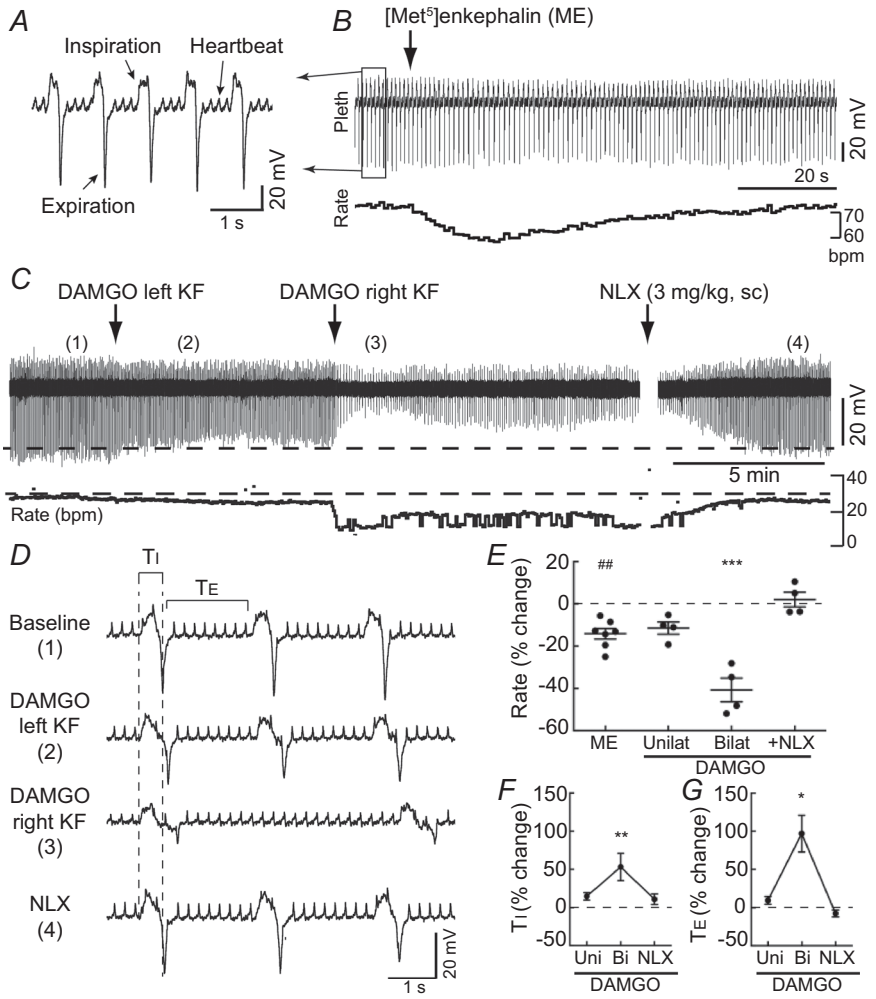

Figure 1. Opioid injection into KF depressed respiratory rate in anaesthetized rats
Respiration was monitored in anaesthetized rats by inductance plethysmography. *A*, respiratory inductance plethysmography recording from boxed area in *B*. Changes in abdominal cavity volume during inspiration and expiration were detected for each breath. *B*, injection of opioid agonist ME (300 pmol) into the KF transiently reduced respiratory rate. Respiratory rate (below) was calculated from the plethysmography (Pleth) recording (above). bpm, breaths min^{-1}. *C*, injection of peptidase-resistant μ opioid agonist DAMGO (60 pmol) into KF (left, then right side) produced long-lasting reduction of respiratory amplitude and rate. Opioid antagonist naloxone (NLX; 3 mg kg^{-1}, s.c.) reversed the effects of DAMGO. Instantaneous respiratory rate (below) was determined from the plethysmography recording (above). *D*, sections of the plethysmography recording in *C* (location indicated by numbers in parentheses) shown on an expanded time-scale. Bilateral DAMGO (3) increased inspiratory time (T_I) and expiratory time (T_E). *E*, summary of the change in respiratory rate from baseline (% change) induced by ME (unilateral) or DAMGO (unilateral and bilateral) injections into the KF. Naloxone (NLX) was administered (3 mg kg^{-1}, s.c.) after bilateral DAMGO injection. Each data point represents an individual injection; line and error bar represent mean ± SEM. *F* and *G*, summary of the change in T_I (*F*) and T_E (*G*) from baseline (% change) induced by DAMGO injections (unilateral and bilateral) into KF and subsequent NLX (3 mg kg^{-1}, s.c.). For ME injections, n = 7 unilateral injections (5 rats). For DAMGO injections, n = 4 rats. $^{\#\#}P < 0.01$ compared to baseline by paired t test. $^{*}P < 0.05$, $^{**}P < 0.01$, $^{***}P < 0.001$ compared to baseline by repeated measures one-way ANOVA and Bonferroni's post-test. Statistics were performed on raw data, but illustrated as normalized data for clarity.

by paired t test), as described previously (Chamberlin & Saper, 1994). After bilateral identification of the KF, the endogenous opioid agonist ME (5 mM, 60 nl) was microinjected into the KF using the same stereotaxic coordinates. Unilateral injection of ME produced a transient reduction in respiratory rate (Fig. 1*B* and *E*; $n = 7$ injections (5 rats)). There was no change in the relative respiratory amplitude following ME injection (98 ± 4% of baseline; $P = 0.81$). Injection sites were marked with fluorescent beads (FluoSpheres 505/515 (10%)), which were included in the pipette with ME (Fig. 3*A*). Injections that were medial, rostral or caudal to the KF had no effect (Fig. 3*A* and *B*; $n = 6$ injections). Injection of FluoSpheres (10%) in saline had no effect on respiratory rate or relative amplitude ($n = 4$ injections).

ME is rapidly degraded by endogenous peptidases, which were not inhibited. When the peptidase-resistant μ opioid agonist DAMGO (1 mM, 60 nl) was injected unilaterally into the KF/lateral PB ($n = 4$ rats), respiratory rate was slightly slowed, which was similar to the reduction induced by unilateral injection of ME (Fig. 1*C* and *E*). Subsequent injection of DAMGO (1 mM, 60 nl) into the KF on the contralateral side resulted in a significant reduction in respiratory rate (41 ± 6% reduction ($P < 0.001$), Fig. 1*C* and *E*) and amplitude (41 ± 7% reduction ($P < 0.001$), Fig. 1*C*). The effects of bilateral DAMGO injection into the KF were reversed by systemic administration of opioid antagonist naloxone (NLX) (3 mg kg^{-1}, S.C.; Fig. 1*C* and *E*). Within 5 min of naloxone injection, respiratory rate and amplitude had returned to baseline levels (102 ± 4% and 94 ± 5% of baseline, respectively; $P > 0.05$ for both). Visualization of FluoSpheres confirmed that bilateral injections targeted the KF (Fig. 3). Thus, activation of opioid receptors in the KF/lateral PB was sufficient to reduce respiratory rate in anaesthetized rats, as previously reported for cats and dogs (Hurlé *et al.* 1985; Prkic *et al.* 2012).

Reductions in respiratory rate can result from increases in inspiratory time (T_I) or expiratory time (T_E). T_I and T_E were measured after DAMGO injections into KF. Bilateral injection of DAMGO increased T_I by 53 ± 18% and increased T_E by 97 ± 24% over baseline (Fig. 1*D*, *F* and *G*). Systemic administration of naloxone (3 mg kg^{-1}, S.C.) reversed the increase in T_I and T_E. Thus, bilateral injection of DAMGO into the KF increased both T_I and T_E, but the large decrease in respiratory rate was mainly due to increases in T_E, similar to previous studies in dogs (Prkic *et al.* 2012).

DAMGO injection into KF causes apneusis in the *in situ* rat preparation

Among the parabrachial areas, the KF is required for the maintenance of a eupnoeic respiratory pattern by initiating the inspiratory to expiratory phase transition (Lumsden, 1923; Fung & St-John, 1995; Dutschmann & Herbert, 2006; Smith *et al.* 2007). The effect of μ opioid receptor activation in KF on the respiratory pattern was studied in the *in situ* arterially perfused working heart–brainstem preparation of rat ($n = 7$ rats; hereafter referred to as the *in situ* preparation) (Paton, 1996; St-John & Paton, 2000). The *in situ* preparation produces a eupnoeic-like respiratory cycle and is advantageous for studying post-inspiratory mechanisms due to KF activity since feedback from pulmonary stretch receptors is removed. The respiratory cycle was monitored by recording simultaneously from the phrenic nerve (PN), which innervates the diaphragm, and the central vagus nerve (cVN), which branches to innervate laryngeal muscles that control upper airway resistance. The phrenic nerve displayed augmenting discharge lasting 0.64 ± 0.04 s, which marked the inspiratory period. The central vagus nerve was active during inspiration, peaked sharply at the termination of inspiration, gradually declined during post-inspiration (post-I) and was silent during stage 2 of expiration (E2) (Fig. 2*B*, Baseline). Measurements of respiratory rate (cycles min^{-1}), phrenic nerve amplitude, and duration of inspiration (T_I), expiration (T_E), post-inspiration (post-I) and stage 2 expiration (E2) were made from the integrated PN and cVN recordings (see Methods).

The KF was again functionally identified by microinjection of glutamate (5 mM, 30–60 nl), which caused a post-inspiratory apnoea (pause in phrenic nerve firing and simultaneous increase in vagus nerve activity), as described previously (Dutschmann & Herbert, 2006). After bilateral identification of the KF, the μ opioid agonist DAMGO (1 mM, 30–60 nl) was microinjected into the KF using the same stereotaxic coordinates (Fig. 2*A* and *B*). Injection of DAMGO into the KF caused a loss of post-inspiration, lengthening of inspiration, reduction of phrenic nerve burst amplitude and an increase in variability of respiratory rate. The most prominent changes induced by unilateral DAMGO injection were the loss of post-inspiratory activity of the vagus nerve (Fig. 2*B* and *C*) and increase in T_I (Fig. 2*B* and *D*). Following subsequent bilateral injection of DAMGO, post-inspiration was abolished and the duration of inspiration was further increased (Fig. 2*B*, *C* and *D*). In addition, the augmenting discharge of the phrenic nerve was converted into a square wave pattern (Fig. 2*B*). The vagus nerve continued to fire during inspiration only and was synchronous with phrenic nerve activity. The amplitude of phrenic nerve discharge was reduced following bilateral DAMGO injection (Fig. 2*A*, bilateral DAMGO = 65 ± 6% of baseline ($P < 0.05$), NLX = 107 ± 6% of baseline ($P > 0.05$)). Together, the lengthened low amplitude inspiration and loss of post-inspiration are characteristic of a respiratory disturbance known as apneusis.

Unlike anaesthetized rat experiments, average respiratory rate did not change (Fig. 2*A*, baseline = 17.1 ± 1.1 cycles min^{-1}, unilateral DAMGO = 17.9 ± 1.3 cycles min^{-1}, bilateral DAMGO = 14.7 ± 1.6 cycles min^{-1}, NLX = 19.1 ± 1.6 cycles min^{-1}, $P > 0.05$ for all). This is likely because expiratory duration (T_E) did not significantly change (baseline = 3.0 ± 0.19 s, unilateral DAMGO = 2.2 ± 0.15 s, bilateral DAMGO = 2.7 ± 0.36 s, NLX = 2.7 ± 0.3 s, $P > 0.05$ for all), and T_E accounted for the majority (82 ± 0.7%) of the total respiratory cycle. However, rate, T_I and T_E all became highly variable after DAMGO injection. The coefficient of variation (CV) for respiratory rate (Fig. 2*A* and *E*) and T_I significantly increased after unilateral and bilateral DAMGO injection (T_I CV: baseline = 8.4 ± 1.5%, unilateral DAMGO = 17.8 ± 3.0% ($P < 0.05$), bilateral DAMGO = 26.7 ± 2.9% ($P < 0.0001$), NLX = 7.5 ± 1.4% ($P > 0.05$)). The CV for T_E significantly increased after bilateral DAMGO injection (T_E CV: baseline = 13.7 ± 1.5%, unilateral DAMGO = 23.3 ± 2.6% ($P > 0.05$), bilateral DAMGO = 32.9 ± 4.3% ($P < 0.001$), NLX = 15.5 ± 2.2% ($P > 0.05$)). The expiratory phase contains both post-inspiration and stage 2 expiration (E2). Not surprisingly, since total expiration did not change and post-inspiration was eliminated, there was an increase in E2 duration following DAMGO injection

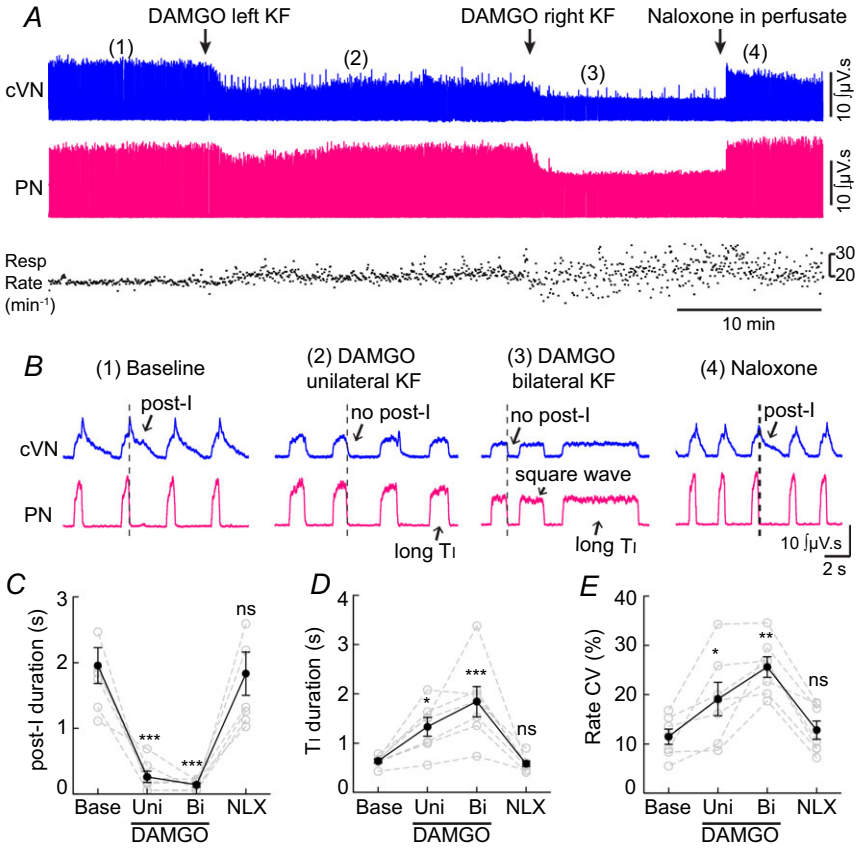

Figure 2. Opioid injection into KF produced apneusis
Recordings from central vagus nerve (cVN) and phrenic nerve (PN) were made using an *in situ* preparation of rat (see Methods). *A*, continuous recording of integrated cVN (top) and PN (bottom) activity. Instantaneous respiratory rate (min^{-1}) is shown below. Injection of μ opioid agonist DAMGO (60 pmol) into KF (left, then right side) rapidly produced sustained alteration in cVN and PN activity. Addition of opioid antagonist naloxone (1 μM) to the reperfusion solution rapidly reversed the effects of DAMGO. *B*, expanded time scale of integrated cVN and PN activity during the experiment shown in *A* (location of sweep indicated by numbers in parentheses). (1) Baseline, a eupnoea-like respiratory rhythm was observed with augmenting PN discharge and post-inspiratory (post-I) cVN activity. (2) Unilateral injection of DAMGO (60 pmol) into the KF reduced post-I and increased inspiratory time (T_I). (3) Bilateral injection of DAMGO (60 pmol) eliminated post-I, further increased T_I, reduced PN amplitude and caused a square wave PN burst, consistent with apneusis. (4) After naloxone (1 μM) was added to the perfusate, post-I cVN activity, augmenting PN discharge and T_I returned to baseline. *C–E*, post-inspiratory duration, inspiratory (T_I) duration, and coefficient of variation (CV) of respiratory rate were calculated for at least 50 respiratory cycles for each condition per rat. Grey symbols are the average for each individual rat; black symbols are group means ± SEM, $n = 7$ rats. $^*P < 0.05$, $^{**}P < 0.01$, $^{***}P < 0.001$, ns = not significant by repeated measures one-way ANOVA and Bonferroni's post-test of raw data.

(baseline = 1.0 ± 0.2 s, unilateral DAMGO = 1.9 ± 0.2 s ($P < 0.05$), bilateral DAMGO = 2.6 ± 0.3 s ($P < 0.0001$), NLX = 0.8 ± 0.1 s ($P > 0.05$)). There was no effect on heart rate (baseline = 391 ± 19 beats min^{-1}, unilateral DAMGO = 393 ± 22 beats min^{-1}, bilateral DAMGO = 390 ± 22 beats min^{-1}, NLX = 396 ± 19 beats min^{-1}, $P > 0.05$ for all). Importantly, all of the effects of DAMGO were rapidly reversed by addition of the opioid antagonist naloxone (NLX; 1 μM) to the reperfusion solution (Fig. 2*A* and *B*) to a level not significantly different from baseline (Fig. 2*C*, *D* and *E*).

One concern may be that DAMGO injections spread to distant brain areas. Injections of DAMGO (1 mM, 60–90 nl, bilateral) that were medial and/or caudal to the KF by < 1 mm did not cause apneusis ($n = 3$). Injection of a lesser amount of DAMGO (0.1 mM, 60–90 nl, bilateral, $n = 4$) into the KF also eliminated post-inspiration (baseline = 2.1 ± 0.3 s; DAMGO = 0.20 ± 0.03 s, $P < 0.01$), increased T_I (baseline = 0.92 ± 0.14; DAMGO = 1.95 ± 0.34 s, $P < 0.05$) and reduced the amplitude of phrenic nerve firing to 74 ± 7% of baseline ($P < 0.01$). These effects were all reversed by injection of naloxone (0.1 mM, 60–90 nl, bilateral, $n = 4$) into the KF at the same site (post-I = 1.61 ± 0.32 s; $T_I = 0.98 \pm 0.12$ s; PN amplitude = 105 ± 9% of baseline; $P > 0.05$ compared to baseline for all parameters). Finally, perfusion of naloxone (1 μM) did not produce any additional changes, indicating that DAMGO had not spread to distant brain areas (post-I = 2.22 ± 0.68 s; $T_I = 0.77 \pm 0.06$ s; PN amplitude = 106 ± 8% of baseline; $P > 0.05$ compared to baseline or to bilateral NLX for all parameters).

Opioids hyperpolarize and reduce excitability of KF neurons

The apneusis caused by microinjection of DAMGO into the KF of the *in situ* preparation was similar to the apneusis caused by ablation of the pons or pharmacological silencing of the KF (Lumsden, 1923; Fung & St-John, 1995;

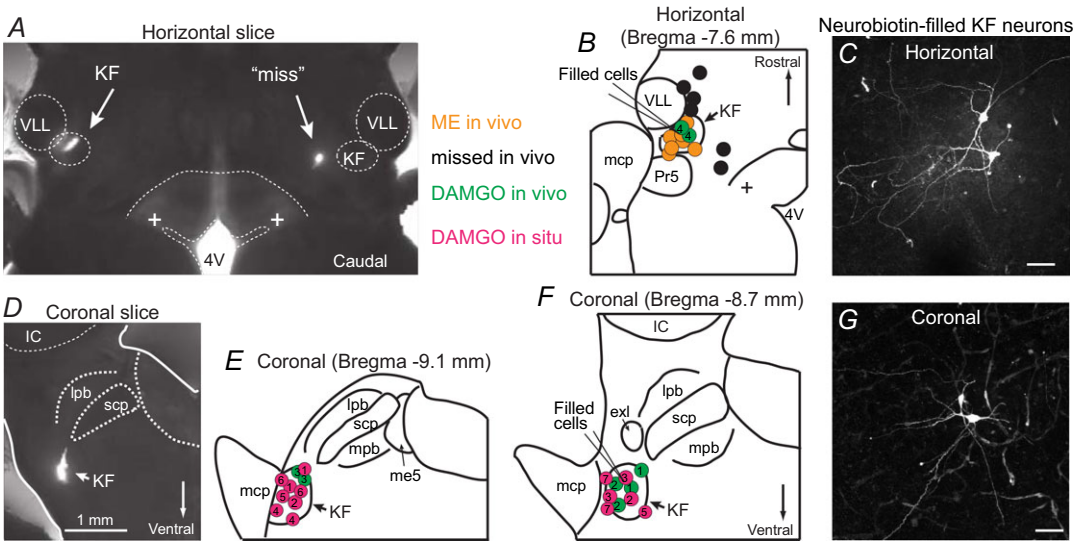

Figure 3. KF neurons were identified in coronal and horizontal slices
A, image of a horizontal slice containing FluoSpheres 505/515 (10%) from a correctly placed KF injection of ME *in vivo* (left side) and a missed injection (right side). *D*, image of a coronal slice containing FluoSpheres (10%) from a correctly placed KF injection of DAMGO. *B*, *E* and *F*, semi-schematic drawings of horizontal (*B*) and coronal (*E* and *F*) slices through rat pons containing KF area. Each drawing is half of a slice with midline at the right edge. Locations of KF injections are mapped by experiment. ME injections (orange; $n = 7$ injections in 5 rats) and missed ME injections (black; $n = 6$ injections) in anaesthetized rat experiments were identified in horizontal slices. DAMGO injections in anaesthetized rats (green) were identified in horizontal and coronal slices ($n = 4$ rats). DAMGO injections in the *in situ* preparation (pink) were identified in coronal slices ($n = 7$ rats). Bilateral DAMGO injections are mapped on the same side; pairs of injections are identified numerically. Brain slice recordings were made from KF neurons in the functionally identified locations. *C* and *G*, KF neurons in coronal and horizontal slices were filled with Neurobiotin (0.1% in the recording pipette) and visualized by confocal microscopy. Locations of the filled cells are indicated above (*B* and *F*). Neurons extended projections similarly in both slice orientations (coronal $n = 7$ cells/3 slices/2 rats; horizontal $n = 9$ cells/5 slices/2 rats). Scale bar = 50 μm. KF, Kölliker–Fuse; scp, superior cerebellar peduncle; lpb, lateral parabrachial area; mpb, medial parabrachial area; exl, external lateral parabrachial area; mcp, middle cerebellar peduncle; me5, mesencephalic 5 nucleus; IC, inferior colliculus; Pr5, principal sensory 5 nucleus; VLL, ventral lateral lemniscus; 4 V, fourth ventricle; +, location of LC in more dorsal slice.

Dutschmann & Herbert, 2006; Smith *et al.* 2007). Since opioids activate Gi/o-coupled receptors, we hypothesized that opioids silence KF neurons by hyperpolarization. To test this, whole-cell recordings were made from KF neurons contained in brain slices.

KF neurons were identified in coronal and horizontal brain slices (Fig. 3). KF neurons were located 0–500 μm ventral to the tip of the superior cerebellar peduncle (scp) in coronal slices corresponding to −8.7 to −9.1 mm caudal from bregma (Fig. 3*E* and *F*). In KF-containing horizontal slices the scp is not present. Instead slices were used that were ventral to the locus coeruleus when the lateral arms of the fourth ventricle were closed, corresponding to −7.6 and −7.8 mm ventral from bregma (Fig. 3*B*). The KF was identified in the rostral–caudal orientation based on its location relative to the ventral lateral lemniscus (VLL). The location was identical to the functionally identified sites in the *in situ* preparation (for coronal slices) or anaesthetized rat (for horizontal slices) (Fig. 3).

KF neurons had similar capacitance, resistance and resting membrane potential in the two slice orientations (C_m = 21.7 ± 0.6 pF coronal (n = 86), 21.4 ± 1.1 pF horizontal (n = 30), P = 0.8 (unpaired t test); R_m = 363 ± 16 MΩ coronal (n = 96), 324 ± 15 MΩ horizontal (n = 52), P = 0.21 (Mann–Whitney test); RMP = −67 ± 0.7 mV coronal (n = 92), −67 ± 0.9 mV horizontal (n = 45), P = 0.43 (unpaired t test)). These cell properties were similar to a previous report of KF neurons in coronal slices from rats older than P21 (Kron *et al.* 2007). Imaging of KF neurons filled with Neurobiotin showed that KF neurons projected dendrites similarly in both coronal and horizontal slices (Fig. 3*C* and *G*), consistent with their similar capacitance measurements. In voltage-clamp recordings from KF neurons, bath perfusion of opioid agonist ME induced an outward current (Fig. 4*A*) in 61% of recorded neurons (91 of 148 neurons, see below). The amplitude of the outward current produced by ME (0.3 or 30 μM) was similar in coronal and horizontal slices (0.3 μM ME: 45 ± 6 pA coronal (n = 10), 50 ± 4 pA horizontal (n = 37), P = 0.49 unpaired t test; 30 μM ME: 78 ± 11 pA coronal (n = 9), 83 ± 6 pA horizontal (n = 42), P = 0.70 unpaired t test). Therefore, data from recordings from KF neurons in coronal and horizontal slices were pooled.

In current-clamp (I = 0) recordings, bath perfusion of opioid agonist ME hyperpolarized KF neurons with

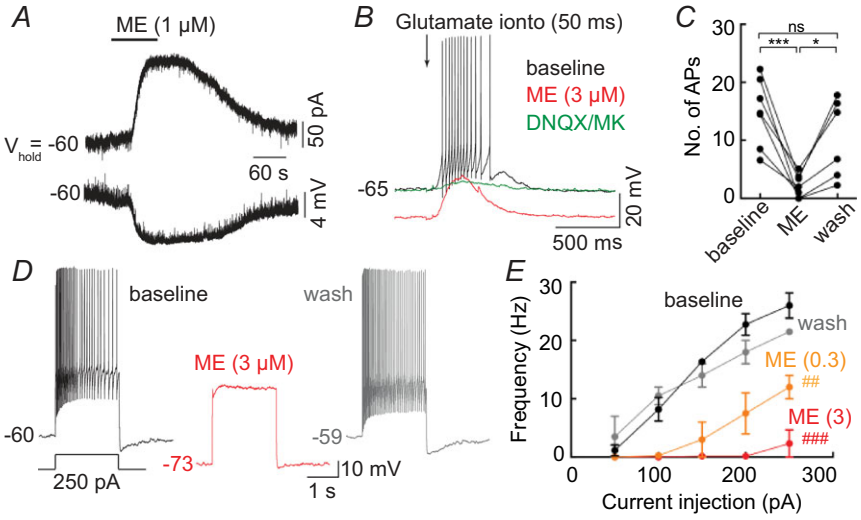

Figure 4. Opioids hyperpolarized and reduced the excitability of KF neurons
Whole cell recordings were made from KF neurons contained in rat brain slices. *A*, bath perfusion of opioid agonist ME (1 μM) produced an outward current in voltage-clamp recordings (top) and a corresponding hyperpolarization in current-clamp recordings (bottom). Resting membrane potential (RMP) of this cell was –60 mV. *B*, current-clamp recording of KF neuron (RMP = −65 mV). Iontophoretic application of glutamate (50 ms) produced action potentials. Bath perfusion of ME (3 μM) hyperpolarized the cell and prevented glutamate-induced firing of action potentials. Depolarization and firing was blocked by perfusion of AMPA and NMDA antagonists DNQX (10 μM) and MK801 (10 μM). *C*, summary of the number of glutamate-induced action potentials (APs) fired at baseline, in ME (3 μM) and after wash. Data from individual experiments are plotted, n = 6–7. $^*P < 0.05$, $^{***}P < 0.001$, ns = not significant by repeated measures one-way ANOVA and Bonferroni's post-test. *D*, injection of current (250 pA) caused firing that decremented in frequency, but persisted for the duration of the current step (2 s). Perfusion of ME (3 μM) hyperpolarized the cell and prevented firing, which reversed when ME was washed from the slice. *E*, summary of firing frequency (average for entire step excluding initial burst of 2–5 APs) by current injection (50–250 pA). Data are means ± SEM, n = 4–5. Bath perfusion of ME (0.3 μM) reduced firing frequency ($^{\#\#}$, two-way ANOVA, $F_{(4,23)}$ = 4.418, $P < 0.01$). Perfusion of ME (3 μM) nearly eliminated firing ($^{\#\#\#}$, two-way ANOVA, $F_{(4,28)}$ = 20.15, $P < 0.0001$). Firing rate after ME wash was not different from baseline (two-way ANOVA, $F_{(4,23)}$ = 1.615, P = 0.20).

a similar time course to the outward current described above (Fig. 4*A*). The average hyperpolarization produced by a near saturating concentration of ME (3 μM) was 10.3 ± 1.3 mV (n = 14). Since hyperpolarization reduces neuronal excitability, the ability of ME to inhibit the firing of KF neurons was tested. None of the KF neurons recorded in whole-cell mode in slices fired spontaneously at rest. However, these neurons did fire action potentials in response to glutamate application or current injection. Local iontophoretic application of glutamate (50–300 ms) caused KF neurons to fire 17 ± 3 action potentials (Fig. 4*B* and *C*). During ME (3 μM) the number of glutamate-induced action potentials was significantly reduced (2.5 ± 0.7 action potentials; Fig. 4*B* and *C*; $P < 0.001$). This inhibition was reversed when ME was washed from the slice (10.3 ± 2.8 action potentials; $P < 0.05$). The inhibition of firing by ME (84 ± 4%) was more effective than simply hyperpolarizing an opioid-sensitive KF neuron by ~10 mV (average bias current = −73 mV), which only inhibited firing by 45 ± 12% (n = 6). AMPA and NMDA receptor antagonists (DNQX, 10–100 μM, and MK801, 10 μM) blocked the depolarization and spiking induced by glutamate iontophoresis (n = 7; Fig. 4*B*).

Positive current steps (50–250 pA) produced firing in KF neurons with increased frequency at larger current steps (Fig. 4*D* and *E*). ME reduced the firing frequency induced by these current steps in a concentration-dependent and reversible manner. At current steps of 250 pA, KF neurons fired at an average frequency of 26 ± 2 Hz. Perfusion of an EC_{50} concentration of ME (0.3 μM) reduced the firing rate to 12 ± 2 Hz ($P < 0.001$, two-way ANOVA and Bonferroni's post-test). A saturating concentration of ME (3 μM) eliminated firing or greatly reduced firing rate evoked by positive current injection (250 pA). When ME was washed from the slice, firing rate returned to a level similar to baseline (22 ± 0.5 Hz; $P > 0.05$, two-way ANOVA and Bonferroni's post-test).

The KF contains a heterogeneous population of neurons based on electrophysiological properties. The opioid-sensitive population of KF neurons made up 61% of all neurons recorded (91 of 148 neurons: 59/96 in coronal slices; 32/52 in horizontal slices). KF neurons that were opioid-sensitive fired with slower frequency in response to current injection (50–250 pA) when compared to KF neurons that were not hyperpolarized by opioids (Fig. 5*A* and *B*; two-way ANOVA, $F_{(1681)} = 409.5$, $P < 0.0001$). Action potentials generated in opioid-sensitive neurons were broader and had a smaller after-hyperpolarization (Fig. 5*C* and *D*). Opioid-sensitive KF neurons also had larger capacitance and lower input resistance (Fig. 5*E* and *F*). However, opioid-sensitive KF neurons did not fire with lower frequency simply due to lower input resistance, as the two parameters were not correlated (R^2 of linear regression = 0.03). Opioid-sensitive and not sensitive neurons had similar resting membrane potentials (Fig. 5*G*). Together, the opioid agonist ME hyperpolarized and reduced the excitability of a large population of KF neurons.

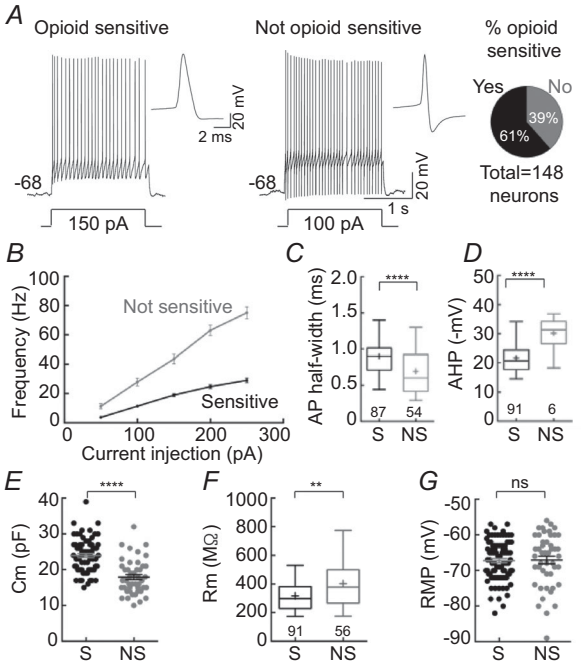

Figure 5. Population of opioid-sensitive KF neurons
Whole cell recordings from KF neurons in brain slice. KF neurons were divided into two populations based on opioid sensitivity as determined by the presence (or absence) of an opioid-mediated hyperpolarizing current (sensitive (S) or not sensitive (NS)). The proportion of KF neurons that were opioid sensitive was 61%. *A*, action potentials recorded during current injection in opioid sensitive (left) or not sensitive neuron (right). Insets, averaged action potential for each neuron during 50, 100 and 150 pA current steps (left = 25 APs; right = 33 APs). *B*, summary of firing frequency by current injection. Data are means ± SEM, n = 56–86. Opioid-sensitive neurons fired significantly slower than not sensitive neurons (two-way ANOVA, $F_{(1681)} = 409.5$, $P < 0.0001$). *C* and *D*, box and whiskers plot of the action potential half-width and after-hyperpolarization of sensitive (S) and not sensitive (NS) KF neurons. Boxes are median and interquartile range ('+' at mean); whiskers are 5–95 percentile; n = 56–87. *E*, *F* and *G*, capacitance, resistance and resting membrane potential of sensitive and not sensitive KF neurons. Data are plotted as individual data points with mean ± SEM (line and error) or as box and whiskers (as above); n = 45–92. $^{**}P < 0.01$, $^{****}P < 0.0001$ by Mann–Whitney test (*C*, *D* and *F*) or unpaired t test (*E*), ns = not significant by unpaired t test. S, opioid sensitive; NS, not opioid sensitive.

μ opioid receptors on KF neurons activate GIRK

Basemed on the previous results, the working hypothesis is that the μ/δ opioid receptor agonist ME hyperpolarizes KF neurons by activating somatodendritic μ opioid receptors that are coupled to G protein-coupled inwardly rectifying

potassium (GIRK) channels. To test this hypothesis, ME was locally applied by iontophoresis (2–3 s), which produced a transient outward current that was very reproducible when applied once every 60 s (Fig. 6*A*). The outward current produced by iontophoresis of ME was blocked by the selective μ opioid receptor antagonist CTAP (1 μM; $n = 3$; Fig. 6*B*). Thus, the ME-mediated current was due to activation of μ opioid receptors.

μ opioid receptors commonly hyperpolarize neurons by activating GIRK channels. To determine the ME-induced current–voltage relationship, voltage ramps (−40 to −140 mV, 500 ms) were applied immediately before and at the peak of an iontophoretic application of ME (Fig. 6*C*). In ACSF containing the standard concentration of extracellular potassium (2.5 mM $[K^+]_o$), the ME-mediated current in KF neurons reversed at −92 mV (Fig. 6*D*), which is near the predicted reversal potential for potassium given the liquid junction potential (10 mV). Increasing the concentration of extracellular potassium shifted the reversal potential as expected for a potassium conductance (−72 mV for 6.5 mM $[K^+]_o$ and −60 mV for 10.5 mM $[K^+]_o$). Higher concentrations of extracellular potassium also increased the conductance of the ME-mediated current, especially the inward conductance. The ME-mediated current was blocked by $BaCl_2$ (100 μM). Together these results indicate that μ opioid receptors hyperpolarize KF neurons by activating GIRK conductance.

Sensitivity to agonists

To determine the sensitivity of μ opioid receptors on KF neurons, various concentrations of ME or the selective μ opioid receptor agonist DAMGO were perfused and the amplitude of the outward current was measured (Fig. 7*A*). The EC_{50} of the ME-mediated current was 226 nM (95% confidence interval (CI): 142–362 nM; Fig. 7*B*), which is similar to the potency of ME in locus coeruleus (LC) neurons ($EC_{50} = 281 \pm 47$ nM; Quillinan *et al.* 2011). The selective μ opioid receptor agonist DAMGO was slightly more potent than ME ($EC_{50} = 90$ nM, 95% CI: 42–192 nM). At saturating concentrations, DAMGO and ME produced the same amplitude current (DAMGO = 77 ± 5 pA ($n = 12$), ME = 82 ± 5 pA ($n = 58$), $P = 0.797$ Mann–Whitney test), which is consistent with full agonist properties of DAMGO and ME and supports the similar effects on rate observed in anaesthetized rat experiments (Fig. 1*E*). The $GABA_B$ agonist baclofen, which also activates GIRK conductance, also produced an outward current in opioid-sensitive neurons. The amplitude of the baclofen (30 μM)-induced current was 68 ± 7 pA ($n = 34$).

Morphine is a partial agonist in many cellular assays. To determine the efficacy of morphine in KF neurons relative to the full agonist ME, saturating concentrations of morphine or ME were perfused and the amplitude of the opioid-mediated current was measured. Saturating concentrations of morphine (10 or 30 μM) produced a current that was 74% of the amplitude of the current

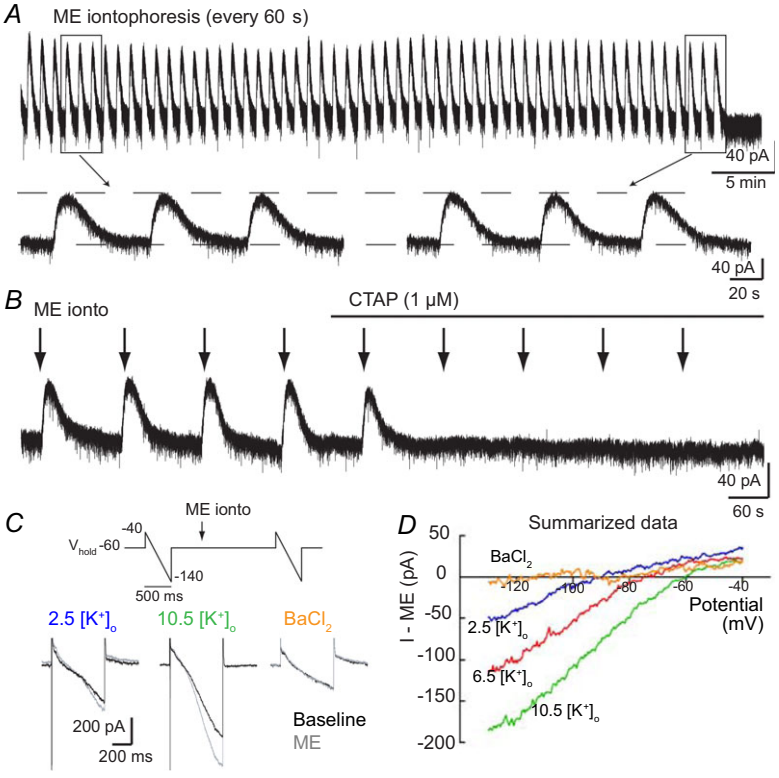

Figure 6. μ opioid receptors on KF neurons activate GIRK
Whole cell voltage-clamp recordings from opioid-sensitive KF neurons. *A*, ME was applied by iontophoresis (7–20 nA, 2–3 s) once every 60 s, which produced a transient, reproducible outward current for up to 1 h. Boxed areas from the beginning and end of the recording are shown on an expanded time scale below. *B*, the ME-induced current was eliminated by perfusion of the selective μ opioid receptor antagonist CTAP (1 μM); $n = 3$. *C*, top, protocol for voltage ramps (−100 mV, 500 ms) applied before and at the peak of ME iontophoresis. Below are representative superimposed traces at baseline (black) and during ME iontophoresis (grey) in normal extracellular potassium (2.5 mM), elevated extracellular potassium (10.5 mM) or with the potassium channel blocker $BaCl_2$ (100 μM). *D*, summary graph of the ME-induced current–voltage relationship in the presence of various extracellular potassium concentrations (mM) or $BaCl_2$ (100 μM). Data are plotted as means; $n = 4$–5 cells.

produced by saturating concentrations of ME (10 or 30 μM), (morphine = 61 ± 7 pA (n = 22), ME = 82 ± 5 pA (n = 58), P = 0.021 Mann–Whitney test). This is consistent with the partial agonist properties of morphine, but is proportionally larger than the morphine-mediated current in LC neurons. In LC neurons, morphine produces a current that is 60% of the amplitude of the current produced by ME (198 ± 28 pA morphine (10 μM; n = 16) *vs.* 349 ± 36 pA ME (30 μM; n = 10); Levitt & Williams, 2012), in agreement with a previous report (Osborne *et al.* 2000). These comparisons between cells are complicated by cell-to-cell variability of GIRK current amplitudes. To provide an intra-cell control for this variability, application of morphine or ME was preceded by application of a low concentration of ME (0.3 μM) (Fig. 7*C*). This pre-application of ME did not alter subsequent opioid-induced currents, as the amplitude of a second application of ME (0.3 μM) was the same as the first application (101 ± 3% of the first application (n = 18), P = 0.66 paired t test). A saturating concentration of morphine (30 μM) produced a current that was 127 ± 10% of the ME (0.3 μM) current, whereas a saturating concentration of ME (30 μM) was 171 ± 7% of the ME (0.3 μM) current (Fig. 7*D*, P = 0.002 unpaired t test), further demonstrating the partial agonist properties of morphine.

To determine the potency of morphine in KF neurons, various concentrations of morphine were perfused and the amplitude of the morphine current was normalized to the amplitude of the current produced by ME (0.3 μM). The EC_{50} of morphine was 406 nM (95% CI: 200–820 nM; Fig. 7*D*). This is similar to the EC_{50} of morphine to activate GIRK in LC neurons (200–600 nM; Osborne *et al.* 2000; Levitt & Williams, 2012).

Discussion

The major findings of this study are that a population of KF neurons were inhibited by μ opioid receptor agonists, including morphine, and activation of μ opioid receptors in the KF suppressed post-inspiratory drive. In anaesthetized, vagi-intact rats, injection of opioid agonists into the KF resulted in a reduction of respiratory rate and amplitude. Bilateral pontine lesions or pharmacological inhibition of the KF in vagi-intact animals produces a similar reduction of respiratory rate (St-John, 1998; Damasceno *et al.* 2014). However, after vagotomy, bilateral pontine lesions or inhibition of the KF causes apneusis (Lumsden, 1923; Fung & St-John, 1995; Dutschmann & Herbert, 2006; Smith *et al.* 2007). In experiments using *in situ* preparations of rat that lack feedback from the vagus,

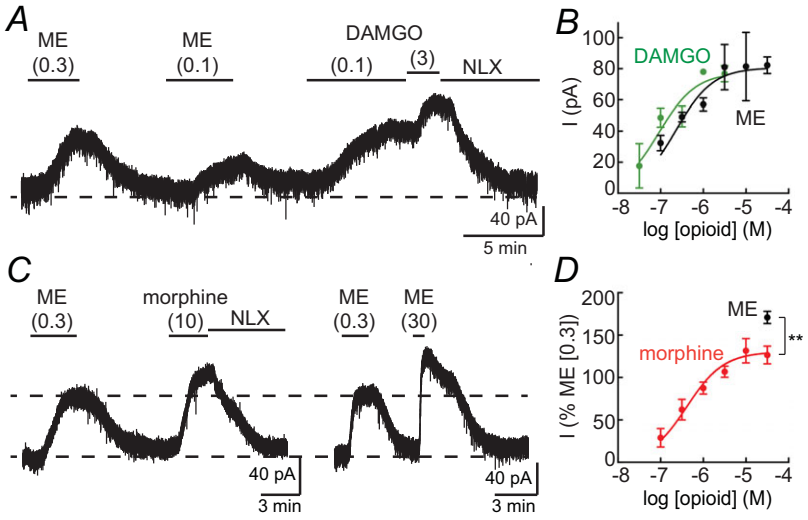

Figure 7. Sensitivity to agonists
Whole cell voltage-clamp recordings from opioid-sensitive KF neurons. *A*, bath perfusion of various concentrations of opioid agonists ME, DAMGO and morphine (μM) were used to determine concentration–response relationships. ME readily washed from the slice. The currents produced by DAMGO and morphine were reversed by the opioid antagonist naloxone (NLX, 1 μM). *B*, concentration–response curves for ME and DAMGO. Data are means ± SEM, n = 3–54 per concentration. EC_{50} of ME = 226 nM (95% CI: 142–362 nM); EC_{50} of DAMGO = 90 nM (95% CI: 42–192 nM). *C*, example recordings of currents produced by saturating concentrations of morphine (10 μM) and ME (30 μM) compared to a low concentration of ME (0.3 μM). *D*, morphine concentration–response curve. The current amplitude produced by morphine (0.1–30 μM) or ME (30 μM) was normalized to the amplitude of the current produced by ME (0.3 μM). Data are means ± SEM, n = 3–11 per concentration. EC_{50} of morphine = 406 nM (95% CI: 200–820 nM). $^{**}P < 0.01$ by unpaired t test.

injection of the μ opioid agonist DAMGO into the KF eliminated post-inspiration and caused apneusis that was comparable to the effect of KF lesion or inhibition.

In brain slice preparations, μ opioid receptors on a distinct population of KF neurons caused a hyperpolarization by activating a GIRK conductance. Opioid agonists activated this conductance with similar potency to their effect in a variety of other midbrain, pontine and medullary areas, including parabrachial (Christie & North, 1988), LC (Christie *et al.* 1987; Osborne & Williams, 1995; Osborne *et al.* 2000; Quillinan *et al.* 2011; Levitt & Williams, 2012), ventral tegmental area (Matsui *et al.* 2014), periaqueductal grey (Chieng & Christie, 1994; Bagley *et al.* 2005), raphe magnus (Pan *et al.* 1990), spinal trigeminal nucleus (Grudt & Williams, 1994), hypothalamic proopiomelanocortin (Pennock & Hentges, 2011), and dorsal root ganglia (Walwyn *et al.* 2009). Circulating concentrations of morphine following systemic treatment are typically in the low micromolar range (Meissner *et al.* 2002; Quillinan *et al.* 2011) and have been reported to be higher (5–10 μM) with doses that cause fatal respiratory depression (Meissner *et al.* 2002). Given the EC_{50} of morphine to hyperpolarize KF neurons (0.4 μM), the expectation is that KF neurons (similar to many other neurons) would be hyperpolarized to some extent during systemic administration of morphine. It is not possible to conclude that the population of KF neurons that are hyperpolarized by μ opioid agonists directly cause the depressant effect of opioids on post-inspiratory activity. However, they are at least likely candidates and may contribute to the respiratory disturbances caused by systemic opioid administration.

Physiological consequence of opioid-induced apneusis

Recurrent laryngeal nerves branch from the central vagus nerves and activate muscles in the larynx that control upper airway resistance. Post-inspiratory activity of these nerves results in activation of laryngeal adductor muscles and increased glottal resistance (Paton & Dutschmann, 2002; Dutschmann & Herbert, 2006). Opioid injection into the KF resulted in loss of post-inspiratory activity of the vagus nerve. Without the increased glottal resistance at the end of inspiration, inhaled air would be rapidly expelled resulting in a suboptimal time for gas exchange and increased risk of lung collapse.

These effects could be compounded by an inability to close the glottis during swallowing or to vocalize properly and coordinate tongue movement (Dutschmann *et al.* 2014; Bautista & Dutschmann, 2014*a*,*b*). In rhythmically active medullary slices, opioids depress the activity of hypoglossal motoneurons by presynaptic inhibition of glutamate release (Hajiha *et al.* 2009; Lorier *et al.* 2010). Clinically, opioids cause aspiration and difficulty in swallowing (Christ *et al.* 2006; Savilampi *et al.* 2013, 2014). Importantly, these effects occurred with doses of remifentanil (0.14 μg kg^{-1} min^{-1}) that only slightly reduced respiratory rate (Savilampi *et al.* 2014), indicating that upper airway impairment occurs with a similar potency to depression of respiratory rate.

Potential phenotype of opioid-sensitive KF neurons

A limitation of the current study is the lack of a direct determination of the phenotype of opioid-sensitive KF neurons. The KF of rats contains a heterogeneous population of inspiratory, post-inspiratory, expiratory and phase-spanning neurons, which are randomly distributed within the KF (Kobayashi *et al.* 2005; Ezure & Tanaka, 2006; Song *et al.* 2006; Dutschmann & Herbert, 2006; Mörschel & Dutschmann, 2009). The percentage of neurons in each category varies considerably between studies but is roughly 40–70% inspiratory, 5–20% expiratory and 20–50% post-inspiratory (very few are non-respiratory). Since opioids in the KF eliminated post-inspiration, one might predict that opioids inhibit post-inspiratory/early-expiratory neurons, which have been shown to initiate post-inspiration (Song *et al.* 2014). This would roughly account for the 61% of opioid-sensitive neurons observed from recordings in brain slice.

The KF is not the only brain region that when silenced eliminates post-inspiration. Inhibition of Bötzinger complex neurons with somatostatin causes nearly identical apneusis (Burke *et al.* 2010). The KF sends dense projections to the Bötzinger complex (Song *et al.* 2012), and post-inspiratory activity of Bötzinger complex neurons is lost when the KF is pharmacologically inhibited (Song *et al.* 2014).

Differences between *in vivo* and *in situ* preparations

Activation of opioid receptors in the KF/lateral PB was sufficient to reduce respiratory rate in anaesthetized, vagi-intact rats, as previously reported for vagotomized dogs and cats (Hurlé *et al.* 1985; Prkic *et al.* 2012). Changes in respiratory rate and amplitude are indicators of respiratory drive, but provide only limited information on the mechanistic effects of opioids on the control of respiration. Experiments in anaesthetized rats were complemented with experiments using the *in situ* preparation. The *in situ* preparation has the advantage of allowing the details of a eupnoeic-like respiratory cycle to be studied in the absence of anaesthetics with an intact brainstem respiratory circuit. Additionally, blood gases are clamped so that experimentally induced changes in respiratory pattern do not result in potentially

confounding reflex responses due to changes in blood gas composition. Activation of μ opioid receptors in the KF of the *in situ* preparation eliminated post-inspiration and increased inspiration (consistent with *in vivo* experiments) with no significant change in expiration or rate.

Feedback from pulmonary stretch receptors is missing from the *in situ* preparation since the lungs are removed. In fully intact conditions, pulmonary stretch receptors provide feedback through vagus nerves to initiate post-inspiration (Feldman *et al.* 1992; Cohen & Shaw, 2004; Molkov *et al.* 2013). The KF may serve as a redundant safety mechanism in case this feedback is altered or desensitized. Apneusis is the result of the loss of the inspiratory off-switch, which is mediated by these two pathways (Lumsden, 1923; Feldman *et al.* 1992). Thus, apneusis following pontine lesions is more pronounced in vagotomized animals (St-John, 1998). The apneusis observed following opioid inhibition of the KF in the *in situ* preparation was more pronounced than in anaesthetized rats. Instead, in vagi-intact anaesthetized rats, the main effect of opioid injection into KF was reduction of respiratory rate, which was similar to the effect of bilateral lesion of the pons or inhibition of the KF reported previously in vagi-intact animals (St-John, 1998; Damasceno *et al.* 2014). Alternatively, it is possible that changes in respiratory rate were not observed in the *in situ* preparation due to occlusion by vasopressin, which can activate V_{1a} receptors in the rostral ventrolateral medulla to increase respiratory frequency and amplitude (Kc *et al.* 2002; Prabha *et al.* 2011).

Location of opioid injections and recordings

The location of the KF was functionally identified before opioid microinjection and confirmed by histology after the experiment. Positive injections were centred in the KF. The nearest neighbours to the KF are the other parabrachial subnuclei, especially the external lateral PB. In anaesthetized rat experiments, there was some diffusion of fluorescent beads up the injection tract into the external lateral PB, which does contain μ opioid receptors (Christie & North, 1988). In the *in situ* experiments, glutamate injections did not spread to the lateral PB, since this would cause tachypnoea rather than the observed post-inspiratory apnoea. Previous studies have shown that pharmacological inhibition of the lateral PB had no effect on control of breathing (Dutschmann & Herbert, 2006; Damasceno *et al.* 2014). This suggests that the major effect of opioid microinjections was due to actions in the KF. Recordings from KF neurons were made at locations identical to the functionally identified sites. Opioid-sensitive neurons were also found in the external lateral PB, but were not included in this study.

Multiple opioid sensitive respiratory regions

Multiple sites of action for μ opioid agonists have been reported in juvenile and adult rats consistent with the distribution of receptors throughout the brainstem respiratory network (Lonergan *et al.* 2003). In addition to KF, these sites include preBötC, Bötzinger complex, rostral ventral respiratory group, nucleus tractus solitarii, caudal medullary raphe, rostral ventromedial medulla and hypoglossal motor nucleus (Lonergan *et al.* 2003; Zhang *et al.* 2007; Hajiha *et al.* 2009; Lorier *et al.* 2010; Montandon *et al.* 2011; Zhang *et al.* 2011; Phillips *et al.* 2012). The KF projects to most of these regions (Song *et al.* 2012). In addition to hyperpolarizing the soma of KF neurons, opioid receptors on terminals of KF neurons could alter respiration by inhibiting neurotransmitter release in the widespread projection regions as well. For instance, opioid-mediated suppression of hypoglossal motoneuron activity is by presynaptic inhibition of glutamate release (Lorier *et al.* 2010).

In conclusion, the present results provide a mechanism for the respiratory disturbances induced by opioids in the KF, whereby opioids hyperpolarized KF neurons and suppressed post-inspiration. This process may be especially involved in upper airway disturbances caused by opioids (Savilampi *et al.* 2014) that will impact patients with impaired upper airway function, such as sleep apnoea (Walker *et al.* 2007). In this study, the sensitivity of μ opioid receptors on KF neurons to agonists was similar to that of neurons in other brain slice preparations and would be activated by clinically relevant circulating concentrations of morphine. Thus, KF neurons that are hyperpolarized by opioids represent additional mediators of opioid-induced respiratory disturbances.

References

Bagley EE, Chieng BCH, Christie MJ & Connor M (2005). Opioid tolerance in periaqueductal gray neurons isolated from mice chronically treated with morphine. *Br J Pharmacol* **146**, 68–76.

Bautista TG & Dutschmann M (2014*a*). Inhibition of the pontine Kölliker-Fuse nucleus abolishes eupneic inspiratory hypoglossal motor discharge in rat. *Neuroscience* **267**, 22–29.

Bautista TG & Dutschmann M (2014*b*). Ponto-medullary nuclei involved in the generation of sequential pharyngeal swallowing and concomitant protective laryngeal adduction *in situ*. *J Physiol* **592**, 2605–2623.

Burke PGR, Abbott SBG, McMullan S, Goodchild AK & Pilowsky PM (2010). Somatostatin selectively ablates post-inspiratory activity after injection into the Bötzinger complex. *Neuroscience* **167**, 528–539.

Chakravarthy B, Shah S & Lotfipour S (2012). Prescription drug monitoring programs and other interventions to combat prescription opioid abuse. *West J Emerg Med* **13**, 422–425.

Chamberlin NL & Saper CB (1994). Topographic organization of respiratory responses to glutamate microstimulation of the parabrachial nucleus in the rat. *J Neurosci* **14**, 6500–6510.

Chieng B & Christie MJ (1994). Hyperpolarization by opioids acting on mu-receptors of a sub-population of rat periaqueductal gray neurones in vitro. *Br J Pharmacol* **113**, 121–128.

Christ A, Arranto CA, Schindler C, Klima T, Hunziker PR, Siegemund M, Marsch SC, Eriksson U & Mueller C (2006). Incidence, risk factors, and outcome of aspiration pneumonitis in ICU overdose patients. *Intensive Care Med* **32**, 1423–1427.

Christie MJ & North RA (1988). Agonists at mu-opioid, M2-muscarinic and $GABA_B$-receptors increase the same potassium conductance in rat lateral parabrachial neurones. *Br J Pharmacol* **95**, 896–902.

Christie MJ, Williams JT & North RA (1987). Cellular mechanisms of opioid tolerance: studies in single brain neurons. *Mol Pharmacol* **32**, 633–638.

Cohen MI & Shaw C-F (2004). Role in the inspiratory off-switch of vagal inputs to rostral pontine inspiratory-modulated neurons. *Respir Physiol Neurobiol* **143**, 127–140.

Dahan A, Sarton E, Teppema L, Olievier C, Nieuwenhuijs D, Matthes HW & Kieffer BL (2001). Anesthetic potency and influence of morphine and sevoflurane on respiration in μ-opioid receptor knockout mice. *Anesthesiology* **94**, 824–832.

Damasceno RS, Takakura AC & Moreira TS (2014). Regulation of the chemosensory control of breathing by Kölliker-Fuse neurons. *Am J Physiol Regul Integr Comp Physiol* **307**, R57–R67.

Dutschmann M & Herbert H (2006). The Kölliker-Fuse nucleus gates the postinspiratory phase of the respiratory cycle to control inspiratory off-switch and upper airway resistance in rat. *Eur J Neurosci* **24**, 1071–1084.

Dutschmann M, Jones SE, Subramanian HH, Stanic D & Bautista TG (2014). The physiological significance of postinspiration in respiratory control. *Prog Brain Res* **212**, 113–130.

Dutschmann M, Mörschel M, Rybak IA & Dick TE (2009). Learning to breathe: control of the inspiratory-expiratory phase transition shifts from sensory- to central-dominated during postnatal development in rats. *J Physiol* **587**, 4931–4948.

Erbs E, Faget L, Scherrer G, Matifas A, Filliol D, Vonesch J-L, Koch M, Kessler P, Hentsch D, Birling M-C, Koutsourakis M, Vasseur L, Vienante P, Kieffer BL & Massotte D (2015). A mu-delta opioid receptor brain atlas reveals neuronal co-occurrence in subcortical networks. *Brain Struct Funct* **220**, 677–702.

Ezure K & Tanaka I (2006). Distribution and medullary projection of respiratory neurons in the dorsolateral pons of the rat. *Neuroscience* **141**, 1011–1023.

Feldman JL, Windhorst U, Anders K & Richter DW (1992). Synaptic interaction between medullary respiratory neurones during apneusis induced by NMDA-receptor blockade in cat. *J Physiol* **450**, 303–323.

Fung ML & St-John WM (1995). The functional expression of a pontine pneumotaxic centre in neonatal rats. *J Physiol* **489**, 579–591.

Gray PA, Rekling JC, Bocchiaro CM & Feldman JL (1999). Modulation of respiratory frequency by peptidergic input to rhythmogenic neurons in the preBötzinger complex. *Science* **286**, 1566–1568.

Grudt TJ & Williams JT (1994). μ-Opioid agonists inhibit spinal trigeminal substantia gelatinosa neurons in guinea pig and rat. *J Neurosci* **14**, 1646–1654.

Hajiha M, DuBord M-A, Liu H & Horner RL (2009). Opioid receptor mechanisms at the hypoglossal motor pool and effects on tongue muscle activity *in vivo*. *J Physiol* **587**, 2677–2692.

Hurlé MA, Mediavilla A & Flórez J (1985). Differential respiratory patterns induced by opioids applied to the ventral medullary and dorsal pontine surfaces of cats. *Neuropharmacology* **24**, 597–606.

Kc P, Haxhiu MA, Tolentino-Silva FP, Wu M, Trouth CO & Mack SO (2002). Paraventricular vasopressin-containing neurons project to brain stem and spinal cord respiratory-related sites. *Respir Physiol Neurobiol* **133**, 75–88.

Kobayashi S, Onimaru H, Inoue M, Inoue T & Sasa R (2005). Localization and properties of respiratory neurons in the rostral pons of the newborn rat. *Neuroscience* **134**, 317–325.

Kron M, Mörschel M, Reuter J, Zhang W & Dutschmann M (2007). Developmental changes in brain-derived neurotrophic factor-mediated modulations of synaptic activities in the pontine Kölliker Fuse nucleus of the rat. *J Physiol* **583**, 315–327.

Levitt ES & Williams JT (2012). Morphine desensitization and cellular tolerance are distinguished in rat locus ceruleus neurons. *Mol Pharmacol* **82**, 983–992.

Lonergan T, Goodchild AK, Christie MJ & Pilowsky PM (2003). Mu opioid receptors in rat ventral medulla: effects of endomorphin-1 on phrenic nerve activity. *Respir Physiol Neurobiol* **138**, 165–178.

Lorier AR, Funk GD & Greer JJ (2010). Opiate-induced suppression of rat hypoglossal motoneuron activity and its reversal by ampakine therapy. *PLoS One* **5**, e8766.

Lumsden T (1923). Observations on the respiratory centres in the cat. *J Physiol* **57**, 153–160.

Matsui A, Jarvie BC, Robinson BG, Hentges ST & Williams JT (2014). Separate GABA afferents to dopamine neurons mediate acute action of opioids, development of tolerance, and expression of withdrawal. *Neuron* **82**, 1346–1356.

Meissner C, Recker S, Reiter A, Friedrich HJ & Oehmichen M (2002). Fatal versus non-fatal heroin 'overdose': blood morphine concentrations with fatal outcome in comparison to those of intoxicated drivers. *Forensic Sci Int* **130**, 49–54.

Molkov YI, Bacak BJ, Dick TE & Rybak IA (2013). Control of breathing by interacting pontine and pulmonary feedback loops. *Front Neural Circuits* **7**, 16.

Montandon G, Qin W, Liu H, Ren J, Greer JJ & Horner RL (2011). PreBötzinger complex neurokinin-1 receptor-expressing neurons mediate opioid-induced respiratory depression. *J Neurosci* **31**, 1292–1301.

Mörschel M & Dutschmann M (2009). Pontine respiratory activity involved in inspiratory/expiratory phase transition. *Philos Trans R Soc Lond B Biol Sci* **364**, 2517–2526.

Osborne PB, Chieng B & Christie MJ (2000). Morphine-6β-glucuronide has a higher efficacy than morphine as a mu-opioid receptor agonist in the rat locus coeruleus. *Br J Pharmacol* **131**, 1422–1428.

Osborne PB & Williams JT (1995). Characterization of acute homologous desensitization of mu-opioid receptor-induced currents in locus coeruleus neurones. *Br J Pharmacol* **115**, 925–932.

Pan ZZ, Williams JT & Osborne PB (1990). Opioid actions on single nucleus raphe magnus neurons from rat and guinea-pig *in vitro*. *J Physiol* **427**, 519–532.

Paton JF (1996). The ventral medullary respiratory network of the mature mouse studied in a working heart-brainstem preparation. *J Physiol* **493**, 819–831.

Paton JF & Dutschmann M (2002). Central control of upper airway resistance regulating respiratory airflow in mammals. *J Anat* **201**, 319–323.

Paxinos G & Watson C (1998). *The Rat Brain in Stereotaxic Coordinates*, 4th edn. Academic, San Diego, CA, USA.

Pennock RL & Hentges ST (2011). Differential expression and sensitivity of presynaptic and postsynaptic opioid receptors regulating hypothalamic proopiomelanocortin neurons. *J Neurosci* **31**, 281–288.

Phillips RS, Cleary DR, Nalwalk JW, Arttamangkul S, Hough LB & Heinricher MM (2012). Pain-facilitating medullary neurons contribute to opioid-induced respiratory depression. *J Neurophysiol* **108**, 2393–2404.

Prabha K, Balan KV, Martin RJ, Lamanna JC, Haxhiu MA & Dick TE (2011). Chronic intermittent hypoxia-induced augmented cardiorespiratory outflow mediated by vasopressin-V_{1A} receptor signaling in the medulla. *Adv Exp Med Biol* **701**, 319–325.

Prkic I, Mustapic S, Radocaj T, Stucke AG, Stuth EAE, Hopp FA, Dean C & Zuperku EJ (2012). Pontine μ-opioid receptors mediate bradypnea caused by intravenous remifentanil infusions at clinically relevant concentrations in dogs. *J Neurophysiol* **108**, 2430–2441.

Quillinan N, Lau EK, Virk M, von Zastrow M & Williams JT (2011). Recovery from μ-opioid receptor desensitization after chronic treatment with morphine and methadone. *J Neurosci* **31**, 4434–4443.

Savilampi J, Ahlstrand R, Magnuson A & Wattwil M (2013). Effects of remifentanil on the esophagogastric junction and swallowing. *Acta Anaesthesiol Scand* **57**, 1002–1009.

Savilampi J, Ahlstrand R, Magnuson A, Geijer H & Wattwil M (2014). Aspiration induced by remifentanil: a double-blind, randomized, crossover study in healthy volunteers. *Anesthesiology* **121**, 52–58.

Smith JC, Abdala APL, Koizumi H, Rybak IA & Paton JFR (2007). Spatial and functional architecture of the mammalian brain stem respiratory network: A hierarchy of three oscillatory mechanisms. *J Neurophysiol* **98**, 3370–3387.

Song G, Tin C & Poon C-S (2014). Multiscale fingerprinting of neuronal functional connectivity. *Brain Struct Funct*; DOI: 10.1007/s00429-014-0838-1.

Song G, Wang H, Xu H & Poon C-S (2012). Kölliker–Fuse neurons send collateral projections to multiple hypoxia-activated and nonactivated structures in rat brainstem and spinal cord. *Brain Struct Funct* **217**, 835–858.

Song G, Yu Y & Poon C-S (2006). Cytoarchitecture of pneumotaxic integration of respiratory and nonrespiratory information in the rat. *J Neurosci* **26**, 300–310.

St-John WM (1998). Neurogenesis of patterns of automatic ventilatory activity. *Prog Neurobiol* **56**, 97–117.

St-John WM & Paton JF (2000). Characterizations of eupnea, apneusis and gasping in a perfused rat preparation. *Respir Physiol* **123**, 201–213.

Walker JM, Farney RJ, Rhondeau SM, Boyle KM, Valentine K, Cloward TV & Shilling KC (2007). Chronic opioid use is a risk factor for the development of central sleep apnea and ataxic breathing. *J Clin Sleep Med* **3**, 455–461.

Walwyn W, John S, Maga M, Evans CJ & Hales TG (2009). δ receptors are required for full inhibitory coupling of μ-receptors to voltage-dependent Ca^{2+} channels in dorsal root ganglion neurons. *Mol Pharmacol* **76**, 134–143.

Wilson RJ, Remmers JE & Paton JF (2001). Brain stem PO_2 and pH of the working heart-brain stem preparation during vascular perfusion with aqueous medium. *Am J Physiol Regul Integr Comp Physiol* **281**, R528–R538.

Zhang Z, Xu F, Zhang C & Liang X (2007). Activation of opioid μ receptors in caudal medullary raphe region inhibits the ventilatory response to hypercapnia in anesthetized rats. *Anesthesiology* **107**, 288–297.

Zhang Z, Zhuang J, Zhang C & Xu F (2011). Activation of opioid μ-receptors in the commissural subdivision of the nucleus tractus solitarius abolishes the ventilatory response to hypoxia in anesthetized rats. *Anesthesiology* **115**, 353–363.

Additional information

Competing interests

The authors have no competing interests to declare.

Author contributions

All authors contributed to the conception and design of experiments: E.S.L. and A.PA. contributed to the collection and analysis of data: *In situ* preparation experiments were performed at the University of Bristol and Oregon Health & Science University. All other experiments were performed at Oregon Health & Science University. All authors contributed to writing the manuscript and all authors approved the final version of the manuscript.

Funding

This work was supported by the National Institutes of Health National Institute on Drug Abuse (Grants Ro1 DA08163 (J.T.W.), F32 DA33036 (E.S.L.) and K99 DA038069 (E.S.L.)), the National Institute of Neurological Disorders and Stroke (Grant R01 NS069220 (A.P.A. and J.F.R.P.)) and the British Heart Foundation (J.F.R.P.).

Acknowledgements

We thank Dr Chris Ford for comments on the manuscript.